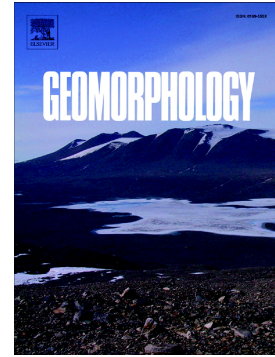# Journal Pre-proof

Climatic controls on the equilibrium-line altitudes of Scandinavian cirque glaciers

Rachel P. Oien, Matteo Spagnolo, Brice R. Rea, Iestyn D. Barr, Robert G. Bingham

Please cite this article as: R.P. Oien, M. Spagnolo, B.R. Rea, et al., Climatic controls on the equilibrium-line altitudes of Scandinavian cirque glaciers, *Geomorphology*(2018), https://doi.org/10.1016/j.geomorph.2019.106986

Climatic controls on the equilibrium-line altitudes of Scandinavian cirque glaciers

Rachel P. Oien[1] (r.oien@abdn.ac.uk)*, Matteo Spagnolo[1] (m.spagnolo@abdn.ac.uk), Brice R. Rea[1] (b.rea@abdn.ac.uk), Iestyn D. Barr[2] (I.Barr@mmu.ac.uk), and Robert G. Bingham[3] (r.bingham@ed.ac.uk)

*corresponding author

[1] University of Aberdeen, School of Geosciences, Department of Geography & Environment, St. Mary's Building, Elphinstone Road, Aberdeen, United Kingdom AB24 3TU

[2] Manchester Metropolitan University, Department of Natural Sciences, Manchester, United Kingdom M1 5GD

[3] University of Edinburgh, School of GeoSciences, Drummond Street, Edinburgh, United Kingdom EH8 9XP

Keywords: equilibrium-line altitude (ELA), Scandinavian cirque glaciers, precipitation, temperature, GIS

Abstract

The equilibrium-line altitudes (ELAs) of reconstructed palaeoglaciers have been widely used to assess palaeoclimatic conditions, yet this concept has rarely been tested using modern glaciers. To address this shortcoming, correlations between the ELAs of 513 modern cirque glaciers and present-day climatic and topographic variables across Scandinavia, as well as regional trends in ELA and climate, are analysed. ELAs are calculated using the Area-Altitude-Balance-Ratio method, with a ratio of 1.5 ± 0.4. Results indicate that glacier ELAs are strongly correlated with distance from the coast. This reflects the present-day precipitation pattern of the region (characterised by high precipitation near the sea) and demonstrates a climate dominated by a maritime-continental transition. Temperature explains differences in glacier ELA regional trends as well as ELA changes with latitude. Following standard meteorological convention, Scandinavia is divided into two macro-

climate regions and analyses are run within the macro-regions as well as the complete dataset. The strength of correlations between ELA and precipitation increases when the study is divided into northern and southern macro-regions. These results test long held assumptions about relationships between climate and cirque glacier ELA, which is of particular relevance to palaeoclimatic studies based on the reconstruction of former cirque glaciers.

1.0 Introduction

Glacier mass balance can be approximated by a single parameter, an equilibrium-line altitude (ELA), which reflects the annual balance between accumulation and ablation (Sutherland, 1984; Ohmura et al., 1992; Benn et al., 2000). Accumulation inputs are precipitation (solid and liquid), avalanching and windblown snow. The accumulation zone is the area of positive mass balance at the end of the mass balance year (typically September in the Northern Hemisphere). Ablation, the process of mass loss, occurs through surface melting, sublimation and, where applicable, submarine melting and iceberg calving. The ablation zone is the area of negative mass balance at the end of the mass balance year. The ELA is the elevation that divides these two zones (i.e., the position of zero annual net mass balance), and is largely determined by local climate (esp. ablation season air temperature and accumulation season precipitation), which exerts a fundamental control on mass balance (Oerlemans and Hoogendoorn, 1989; Ohmura et al., 1992; Benn et al., 2000; Winkler et al., 2009; Rea, 2009; Ohmura and Boettcher, 2018). Perturbations of either one of the two climate variables will impact glacier mass balance and ELA, resulting in either glacier advance or retreat. Due to this relationship, ELAs, or trends therein, can be used as a proxy for climate and/or climate gradients. This is of particular relevance in formerly glaciated regions, where reconstructed ELAs (derived through various methods) are assumed to provide a palaeoclimate proxy (Torsnes et al., 1993; Benn et al., 2000; Carrivick and Brewer, 2004; Barr and Spagnolo, 2015a). For example, cirque floor elevation, which is considered a proxy for cirque glacier ELA, has been used to reconstruct regional palaeo-precipitation and temperature trends (Barr and Spagnolo, 2015b; Barr et al., 2017). However, relatively few studies have conducted a rigorous test of the validity of using ELA trends as a proxy for

2

climate gradients, based on modern glaciers and climate (Rupper and Roe, 2008; Sagredo et al., 2014). Mostly, this is due to a lack of measured (i.e. calculated from long term mass balance field data) ELAs. Recent developments in the availability of high-resolution digital elevation models (DEMs), GIS tools, global inventories of mapped glacier outlines, and global climate data can now be exploited to fill this gap (Braithwaite and Raper, 2009). In this study, we utilise such datasets to investigate relationships between the ELAs of modern cirque glaciers and present-day climate across Norway and Sweden.

2.0 Methods

2.1 Selecting glaciers

Cirque glaciers are abundant, simple in their morphology, and relatively small, therefore they have a short response time and are sensitive to climate forcing (Trenhaile, 1975; Rosqvist and Østrem, 1989; Grudd, 1990; Rudberg, 1994; Fujita, 2008; Winkler et al., 2009). This paper considers only cirque glaciers, i.e. larger ice masses, ice caps, plateau and valley glaciers, were not included. Polygons delineating the perimeters of all of Scandinavia's ~1600 modern glaciers were obtained from the Norwegian Water Resources and Energy Directorate (NVE). These glaciers were mapped from Landsat TM/ETM+ satellite imagery, acquired between 1999 and 2006 (Andreassen et al., 2012; Winsvold et al., 2014), and are part of the GLIMS global glacier database (GLIMS and NSIDC, 2005, updated 2018; Raup et al., 2007). For this study, each glacier was labelled using its unique GLIMS code. Cirque glaciers (n = 513) were identified using the definition by Evans and Cox (1974) and contoured at 15 m intervals using a 10 m resolution DEM (Norwegian Mapping Authority, 2016, Figure 1). We also used Google Earth imagery from the 2006 ablation season to confirm the presence of all cirque glaciers (Figure 2).

2.2 Calculating ELAs

The most accurate way to determine the ELA of a modern glacier is directly from its mass balance, ideally measured for at least 10 consecutive years (Rea, 2009). However, worldwide there

3

are <150 glaciers which have at least 10 years of continuous direct mass-balance measurements (Braithwaite, 2009), none of which are cirque glaciers in Scandinavia. An alternative approach is to derive the ELA from glacier geometry (Trenhaile, 1975; Rosqvist and Østrem, 1989; Grudd, 1990; Nesje, 1992; Torsnes et al., 1993; Osmaston, 2005). We adopt the latter approach, using a GIS tool developed by Pellitero et al. (2015) which only requires a DEM and mapped polygons of glacier perimeters as inputs. While there are different techniques to calculate a glacier ELA (Pellitero et al., 2015), the ELA of the modern 513 Scandinavian cirque glaciers were calculated using the Area Altitude Balance Ratio (AABR) and Accumulation Area Ratio (AAR) methods only, following Rea (2009). Ratios of 1.5 ± 0.4 and 0.58 were selected for the AABR and AAR, respectively, based on the regional values obtained from the analysis of measured ELAs in Scandinavia (Rea, 2009). For the 513 cirque glaciers, the difference between ELAs calculated using the AABR and AAR methods is less than 5 m. Henceforth, for the sake of simplicity, the only ELAs discussed in this paper are those derived using the AABR method.

2.3 ELA validation

While our study focuses on cirque glaciers in Scandinavia, n order to validate this approach, we compared GIS-calculated (using the AABR and AAR methods) and measured ELAs for 11 Scandinavian valley and plateau glaciers. These are the only Scandinavian glaciers ELAs from the World Glacier Monitoring Service (WGMS) that have been derived from measured mass balance records spanning at least 10 years, including the 1999-2006 period, which corresponds to the timeframe of the cirque glacier mapping (Winsvold et al., 2014; Kjøellman, 2017). For each glacier, the zero net mass balance was calculated by plotting the annual specific net balance versus the ELA, following Rea (2009). The GIS-calculated and measured ELAs are highly correlated ($r^2 = 0.99$). The average difference between the GIS-calculated and zero net mass balance measured ELAs is 26.2 m, which is minimal given other uncertainties in mass balance measurements. This indicates that the GIS-calculated ELAs represent good estimates of measured ELAs and are reliable for the analysis of regional trends.

2.4 Comparison with climate

To compare ELAs with climate, we extracted a series of climatic parameters at the ELA of the 513 cirque glaciers and analysed their regional trends. We obtained gridded (1 km x 1 km) precipitation and temperature data from the NVE for the period 1976 to 2006 (http://seNorge.no; Engelhardt et al., 2012; Lussana et al., 2016; Wong et al., 2016). This period was chosen because the glacier outlines were mapped between 1999 and 2006, and we assume their geometry is a function of the climate averaged over the previous 30 years (Andreassen et al., 2012). For temperature, grids of mean summer (JJA) air temperature (Figure 3) and mean annual air temperature (MAAT) were generated. For precipitation, grids of mean winter (DJF) precipitation (Figure 4) and mean annual precipitation were generated. Glacier latitude, aspect, solar radiation and distance from the coast were also considered, since these parameters have previously been suggested, or are known, to have an influence on cirque glacier ELAs (Sutherland, 1984; Rosqvist and Østrem, 1989; Evans, 2006a; Raper and Braithwaite, 2009; Křížek and Mida, 2013; Barr and Spagnolo, 2015a). Aspect was calculated using the ACME ArcGIS tool (Spagnolo et al., 2017). Solar radiation was calculated using the 'area solar radiation' ArcGIS tool, and a mean value was calculated for each glacier. The coast was defined as a manually digitised line that excluded fjords, and the Euclidian distance from each glacier to this line was measured using the 'Near' ArcGIS tool. A midpoint was placed along the ELA contour of each cirque glacier and used to extract temperature, precipitation, and latitude from the relevant gridded datasets.

Climatically, the study region can be divided into two macro-regions: a southern 'temperate', macro-region, influenced by the North Atlantic Current; and a northern 'polar/subpolar' macro-region, proximal to the polar front and Siberia (Tveito et al., 2000). The cirque glacier database can also be divided into northern and southern macro-regions, separated by a major topographic saddle in the Scandinavian mountains. This division, at ~64°N (Figure 1), corresponds approximately to the climatic divide, north of which there are 255 cirque glaciers and south of which there are 258. Given this natural division, analyses were conducted on the entire cirque glacier dataset as well as separately on the two macro-regions. Notably, within the southern macro-region, there is a strong west-east gradient, from a maritime to continental climate. This gradient, while discussed in the Scandinavian glacier literature (e.g. Torsnes, 1993; Nesje et al., 2008; Nesje, 2009; Winkler et al., 2009; Winsvold

5

et al., 2014), does not have a distinct boundary which defines the transition, and therefore the dataset was not subdivided further or defined as its own macro- region. Further climatic subregions might exist and certainly existed in the past, however, these are not considered in the present work, which focuses on how present-day climatic trends are reflected in modern cirque glacier ELAs.

Plots showing regional trends in ELA, elevation, winter precipitation and summer temperature (the two climatic parameters known to affect glacier mass balance the most) were also generated (Figure 7), showing how these variables change with distance from the coast. In order to investigate the regional climates, 10 km-wide swaths parallel to the coastline were constructed. ArcGIS zonal statistics were used to extract minimum, mean and maximum values for each parameter (ELA, elevation, winter precipitation and summer temperature) within each swath. Neither temperature nor precipitation were reduced to sea level, as it is the value at the elevation of the glaciers that matters when it comes to identifying how mass balance and ELA respond to climate. The northern macro-region contains cirque glaciers from 0 km to 150 km from the coast, while the southern macro-region contains cirque glaciers between 30 km and 200 km from the coast. To allow comparison between the two macro-regions, climate and ELA trends were analysed between 30 km and 150 km from the modern coast.

We use the above data to analyse correlations between ELA and all possible controls, then apply Principal Component Analysis (PCA) to explore these relationships further.

3.0 Results

3.1 ELA analysis for the entire dataset

The 513 cirque glaciers analysed in this study cover 200 km of longitude and 1400 km of latitude (Figure 1). The calculated ELAs for these glaciers range from 495 m to 2027 m. The lowest ELAs are found near the coast, primarily in the north, and the highest ELAs are found inland in the south (Figure 3). Taking the dataset as a whole, Pearson correlations between glacier ELA and the other parameters, which have been extracted at the ELA, range from -0.828 to +0.817 (Table 1). The strongest correlation (r = -0.828) is between ELA and mean summer air temperature, and the second

strongest is with distance from the coast ($r = 0.817$) (Table 1). Latitude and MAAT also have strong negative correlations with ELA. Solar radiation is positively, but weakly, correlated with ELA; precipitation is negatively, but weakly, correlated with ELA ($r = -0.187$ for annual, and -0.249 for winter).

3.2 Principal Component Analysis

Using the above data, PCA (Figure 5) supports the finding that distance from the coast and ELA co-vary, as demonstrated by the acuteness of the angle between the two variables. Another important relationship identified from this analysis is that the southern macro-region can be further subdivided into two groups. One of the principal components is distance from the coast, while the other is precipitation, both winter and annual (Figure 5). The PCA of the northern cirque glaciers primarily clusters around the axes of MAAT and mean summer air temperature.

3.3 Macro-region ELA analysis

The strength of the correlation between ELA and air temperature, both MAAT and mean summer, changes little when analysed at the macro-region level. Negative correlations between ELA and MAAT are very strong in both the northern and southern regions (Table 1). Negative correlations between ELA and mean summer air temperature are strong in the northern region and very strong in the southern region (Table 1). Correlations between precipitation and ELA are weak in the northern region ($r = +0.118$ and $+0.105$ for annual and winter totals, respectively) but very strong in the southern region ($r = -0.783$ and -0.790 for annual and winter totals, respectively). The strength of the correlations between ELA and distance from the coast remains comparable to the full dataset in both the northern and southern regions, as do correlations with aspect and solar radiation. The negative correlation between ELA and latitude remains strong in the northern region ($r = -0.505$), while it weakens in the southern region ($r = -0.165$).

3.4 The role of continentality

The entire dataset shows a strong negative correlation between distance from the coast and temperature, both MAAT and mean summer. At the macro-regional scale, the correlation between

7

distance from the coast and MAAT, in both the northern and southern regions, becomes very strongly negative (Table 2). The negative correlation between distance from the coast and mean summer temperature weakens in the northern region (r = -0.431) yet remains strong in the southern region (r = -0.643). Distance from the coast and precipitation are weakly negatively correlated for the whole dataset (r = -0.266 and -0.311, for annual and winter precipitation, respectively). In the northern region, this relationship remains weakly negative (r = -0.142 and -0.107 for annual and winter precipitation, respectively), but is strongly negative in the southern region (r = -0.558 and -0.582 for annual and winter precipitation, respectively).

3.5 Climate trends across Scandinavia

Climate trends in Scandinavia are affected by the presence of the mountain range that extends the length of Norway. The altitudinal effect of topography is reflected in the mass balance of the region's glaciers. Using the buffer zones, regional climatic patterns (not climate at the ELA) could be evaluated using swaths as distance from the coast (Figure 6). With distance from the coast, temperature and precipitation generally decrease, while ELA increases, in both the southern and northern regions.

In the northern region, summer temperature declines inland with a gradient of -0.09℃/10 km and the lowest average summer temperature of 8.76˚C occurs within the interval 110-120 km from the coast. In the southern region, average summer temperature declines inland with a gradient of -0.25℃/10 km, reaching its lowest value of 8.2 °C at 115 km inland, which is the highest topography in the southern Scandinavian Mountains, near Jotunheimen. The lowest average summer temperature in the southern region is 8.22˚C, 100-110 km from the coast. In the northern region, winter precipitation decreases inland with a gradient of -12.9 mm/10 km, and a minimum value of 427.4 mm occurs ~105 km from the coast. In the southern region, winter precipitation decreases inland with a gradient of -39.3 mm/10 km, and a minimum value of 166.8 mm occurs ~205 km from the coast. The mean elevation of topography generally increases inland with a gradient of 39.2 m/10 km in the northern region and 61.0 m/10 km in the southern region. Glacier ELAs show similar patterns, i.e. ELAs increase inland at 44.5 m/10 km and 59.0 m/10 km, in the northern and southern regions, respectively.

8

4.0 Discussion

4.1 Controls on cirque glacier ELAs

Our findings suggest that multiple, sometimes competing, factors influence modern cirque glacier ELAs across Scandinavia. The strong correlation of ELA with distance from the coast likely reflects the competing role of present-day temperature (Figure 3) and precipitation (Figure 4) on glacier mass balance. Both temperature and precipitation decline with distance inland, which would have opposite effects on ELA. The strong rise in ELA with distance inland implies that reduced precipitation exerts the stronger influence, but temperature still plays a role, as demonstrated by the analyses of the two macro-regions (Figure 6). In the south, summer temperature decreases inland at a relatively high rate, mainly caused by rising elevation (Figure 6b). Despite the general decrease in summer temperature inland that would tend to lower the ELA, the ELA increases inland because of the very strong declining precipitation gradient in the southern Scandinavian mountains (Figure 6d), as also noted by others in this same region (Winkler and Nesje, 2009; Winkler et al., 2009; Trachsel and Nesje, 2015). In the north, the winter precipitation gradient inland is much weaker (Figure 6c) but so is the summer temperature gradient (Figure 6a), and the combined effect of the two on glacier mass balance means that the ELA increases inland here, as it did in the south. This general finding mirrors that of Sagredo et al. (2014), who analysed ELA/climate relationships in the Andes. The strong link between precipitation gradients and ELA suggests that continentality, and specifically moisture availability, is a key control on ELA within the Scandinavian mountains. Disparity between continental and maritime climates has long been hypothesised to exert the strongest climatic impact on glacier mass balance globally (Braithwaite, 1984).

While precipitation is the key parameter in determining how glacier ELA changes with distance to the coast, temperature becomes the dominant influence on latitudinal ELA trends. This is demonstrated by the negative correlation between ELA and latitude (Table 1). The larger latitudinal range of the northern region (5.5°) relative to that of the southern region (3°) contributes to the

stronger ELA/latitude correlation in northern Scandinavia (Table 1). The effect of temperature could also be seen in the distribution of cirque glaciers, which is very different between the two macro-regions. More glaciers are found close to the coast in the north than in the south (16.6% vs. 1.2%, within the first 50 km), most likely reflecting the fact that temperatures near the coast are lower in the northern region (Figure 6a).

Several previous studies have highlighted the influence of aspect on cirque glaciation. For example, Evans (2006b; 2011) has demonstrated that in the northern hemisphere, and more specifically in Scandinavia, cirques favour formation in NE aspects. Here, winter accumulation could be accentuated through windblown deposition and melting is suppressed by reduced exposure to solar radiation over diurnal cycles, with the maximum sunlight occurring in the mornings when temperatures are cooler (Chueca and Julián, 2004; Barr and Spagnolo, 2015a). Most of the analysed cirque glaciers are characterised by a NE aspect with a vector mean of 41° (Figure 7). The weak correlation between cirque glacier received solar radiation and ELA, suggests that rather than controlling present-day cirque glacier ELAs, aspect and solar radiation affect sites of glacier initiation—thereby controlling where modern cirque glaciers are located.

Although some of the relationships explored imply that climatic factors strongly influence cirque glacier ELA, a further possibility is that there is a significant direct topographic control, in that high- and low-altitude cirque glaciers can only form where high- and low-altitude topography exist. The distribution of glaciers relative to elevation is an aspect of great relevance for regional studies on glacier ELA because it demonstrates that non-climatic variables, such as topographic availability, might affect cirque glacier distributions. Specifically, climate might determine a theoretical ELA that is higher than the available elevation in a landscape, but glaciers can only be present where there is a landscape on which to form. Within our study, only 19% of the glaciers occur at an elevation that is more than 300 m below the highest surrounding (within 2 km) topography. Regional ELA trends may, in some cases, be limited by topographic availability rather than representing a direct proxy for climate (Anders et al., 2010).

4.2 Implications for palaeoclimate reconstruction

10

For the purpose of palaeoenvironmental reconstruction, it is often assumed that former cirque glacier ELAs are proxies for palaeoclimate (Evans, 2006b; Pearce et al., 2017; Ipsen et al., 2018). This applies to ELAs calculated from three-dimensional palaeoglacier reconstructions, and to more simple estimates of ELAs, for example from cirque-floor altitudes (Benn et al., 2000; Barr and Spagnolo, 2015a). This has also been applied to palaeoenvironmental studies where distance from the coast has been used as a proxy for palaeoprecipitation and linked to changes in palaeoglacier ELAs (Barr and Spagnolo, 2015b).

Results from this study, which focuses on modern cirque glaciers and present-day climate, support the idea that cirque ELA is controlled by climate, and is therefore, a valid palaeoclimatic proxy, but with a few caveats. For example, our study has demonstrated clear regional (northern vs. southern Scandinavia) differences in controls on ELA. Importantly, there are a number of parameters where the strength of correlation changes considerably depending on the size of the study area. For example, the correlation between precipitation, especially winter, and ELA changes from very weak, for the whole dataset, to very strong, for the southern region. The geographical split of the dataset into two regions was dictated by knowledge of present-day Scandinavia climate, characterised by the presence of two major climatic zones ('polar/subpolar' in the north and 'temperate' in the south) (Tveito et al., 2000). The North Atlantic Oscillation controls a large amount of winter precipitation throughout Scandinavia (Hanssen-Bauer, 2005). The North Atlantic Current, which extends to the Norwegian Current, creates a milder climate than expected at such high latitudes. The climatic distinction between these two zones was further confirmed by the PCA which clearly identifies the two regions based on a primary climate variable and subgroups within those regions. However, all this information was only available to us because we were dealing with present-day climate. In a palaeoclimate context, splitting glacier populations on the basis of assumed palaeoclimate differences is non-trivial, and possibly circular, since the aim of such studies is often to use palaeoglacier ELAs to reconstruct former climate. Therefore, one recommendation from this study is that in order to interpret palaeo ELA trends, datasets covering large regions, with the potential to extend over multiple climatic zones, should be sub-divided in multiple ways, to highlight potential sub-populations (i.e. ELA

11

gradients should be analysed on a regional basis) (Evans, 2006a; Barr and Spagnolo, 2015a). In the first instance this sub-division should be guided by obvious physiographic characteristics. Additional information regarding past climate, which could be extracted from other proxies such as tree rings, speleothems (cave deposits) and lacustrine and marine deposits which contain foraminifera, pollen, diatoms, microfossils and chironomids (e.g. Kellogg, 1977; Mangerud et al., 1981; Laurizten, 1995; Hertzberg and Schmidt, 2006; Baker, 2009; Skoglund and Laurizten, 2010; Bakke et al., 2013; Olsen et al., 2013; Jansen et al., 2016), could also prove useful in guiding a regional analysis. However, caution should be applied when using other proxies to define regional climates to ensure they do not compromise subsequent palaeoprecipitation calculations derived from the ELAs i.e. circularity should be avoided.

The present study focuses on cirque glacier ELAs at a fixed point in time (i.e. the present), however, studies which use cirque-floor altitudes as a proxy for palaeoclimate often ignore the time transgressive nature of their occupation. In Figure 7, there is a swath of topography which is currently occupied by cirque glaciers, from a minimum elevation generally to the highest elevation at which topography allows a cirque to exist. There are in many instances un-occupied cirques below the present-day minimum elevation, because temperature is too high. As climate changes this lower limit to glaciation migrates most likely in response to temperature, unless there is a major change in precipitation. When climate is warmer the cirque-occupation swath becomes increasingly limited by topographic availability. Conversely as climate cools the minimum elevation for cirque-occupation lowers and the swath elevation range increases with, at some point, higher elevation cirque glaciers expanding and coalescing to form valley glaciers. When assessing a deglaciated landscape, using cirques as a paleoclimate proxy, all cirques are grouped, ignoring the time transgressive nature of their occupation. Further work is required to assess how best to interpret the paleoclimate signal from a landscape-scale analysis of cirques, but the gradient in minimum cirque elevation is most likely to represent a temporally coherent dataset.

5.0 Conclusions

We used ArcGIS, high-resolution mapping and present-day climate to assess the relationships between modern cirque glacier ELAs and climate, with a focus on Scandinavia. The most significant findings are:

- One of the strongest relationships is between ELA and distance from the coast, with ELA increasing inland. This reflects the strong maritime-continental transition that characterises the region. The correlation between the two parameters most likely results from a relatively strong precipitation gradient coupled with a weak temperature gradient in the south, and a weaker precipitation gradient coupled with a weaker temperature gradient in the north. This illustrates the competing effect of temperature and precipitation on glacier ELA.

- The strength of a number of correlations between modern glacier ELA and present-day climatic and topographic parameters changes depending on the extent of the study area (Scandinavia versus two smaller macro-regions). This highlights the importance of regional climate variability in controlling ELA trends and it is of particular relevance to palaeoglacier reconstructions because the data with which to define regional differences will be limited and may be the target of the glacier reconstructions. Bigger is not necessarily better and it is recommended that large datasets also be analysed as subsets, defined by physiographic and/or other paleoclimate proxies. Caution should be applied to avoid circularity if palaeoprecipitation is to be calculated.

- If assessing a landscape of un-occupied cirques for paleoclimate interpretation, care must be taken to consider the time transgressive nature of cirque occupation. The gradient in minimum cirque elevation is most likely to represent a temporally coherent dataset.

- Topographic availability matters: if there is no topography at the theoretical ELA, glaciers cannot form, and this might affect apparent ELA-climatic gradients.
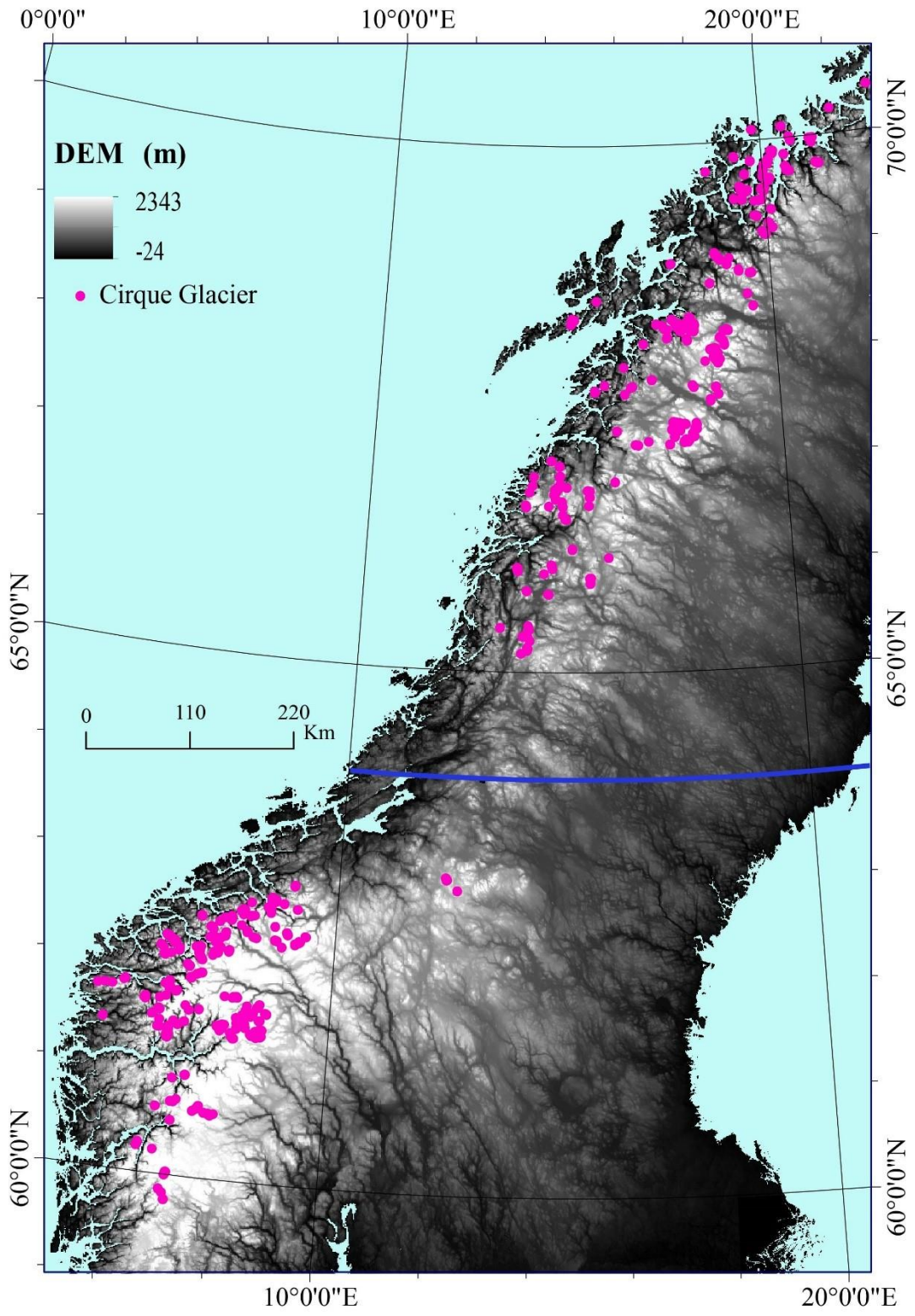
6.0 Acknowledgements

7.0 Figures

Figure 1: Locations of cirque glaciers analysed within this study (pink dots). The topographic saddle at ~64˚N coincides with a latitudinal change in climatic zones. The thick blue line separates the two macro-regions discussed in the text.
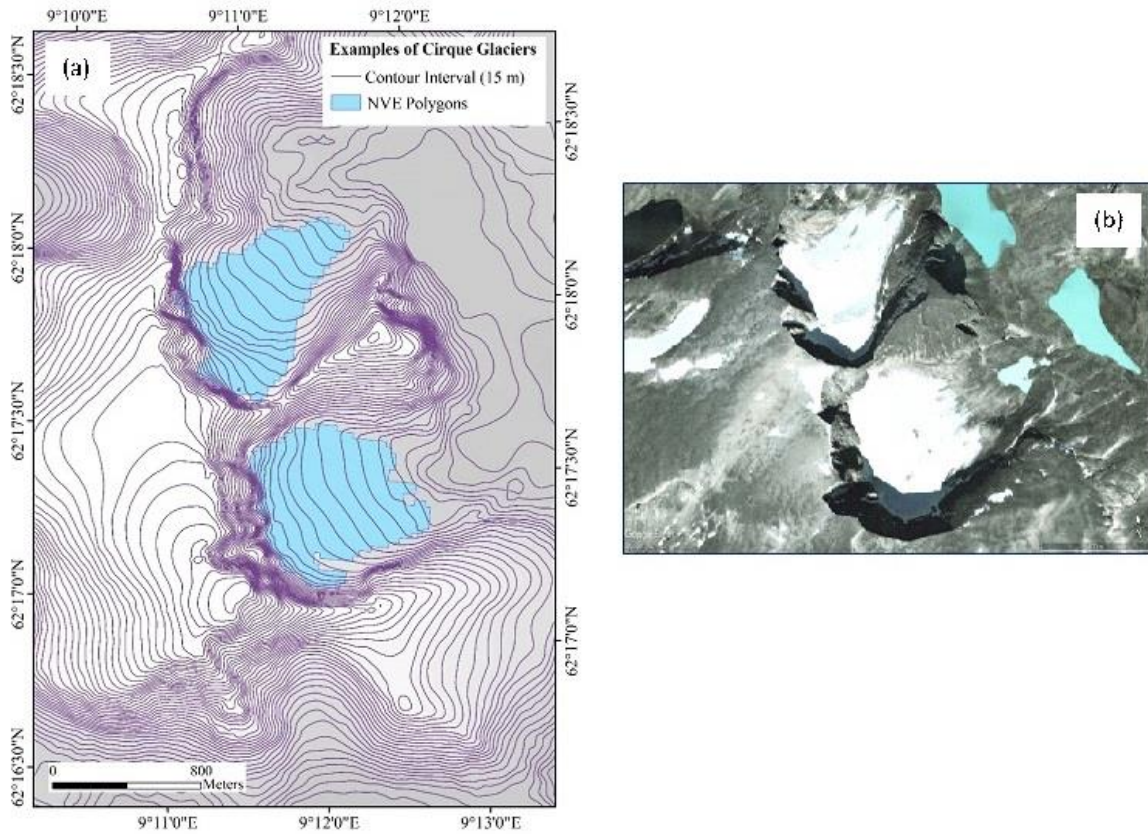

Figure 2: Example of two cirque glaciers analysed in this study. (a) Cirque glacier polygons obtained from the NVE. Also shown are 15 m elevation contours derived from the NVE DEM. (b) The same area viewed in a Google Earth image from the end of the ablation season in 2006, used to verify the presence of these glaciers. The top glacier is GLIMS ID G009186E62298N and the bottom glacier is GLIMS ID G009194E62289N location near the mountain Storstyggesvånåtinden.
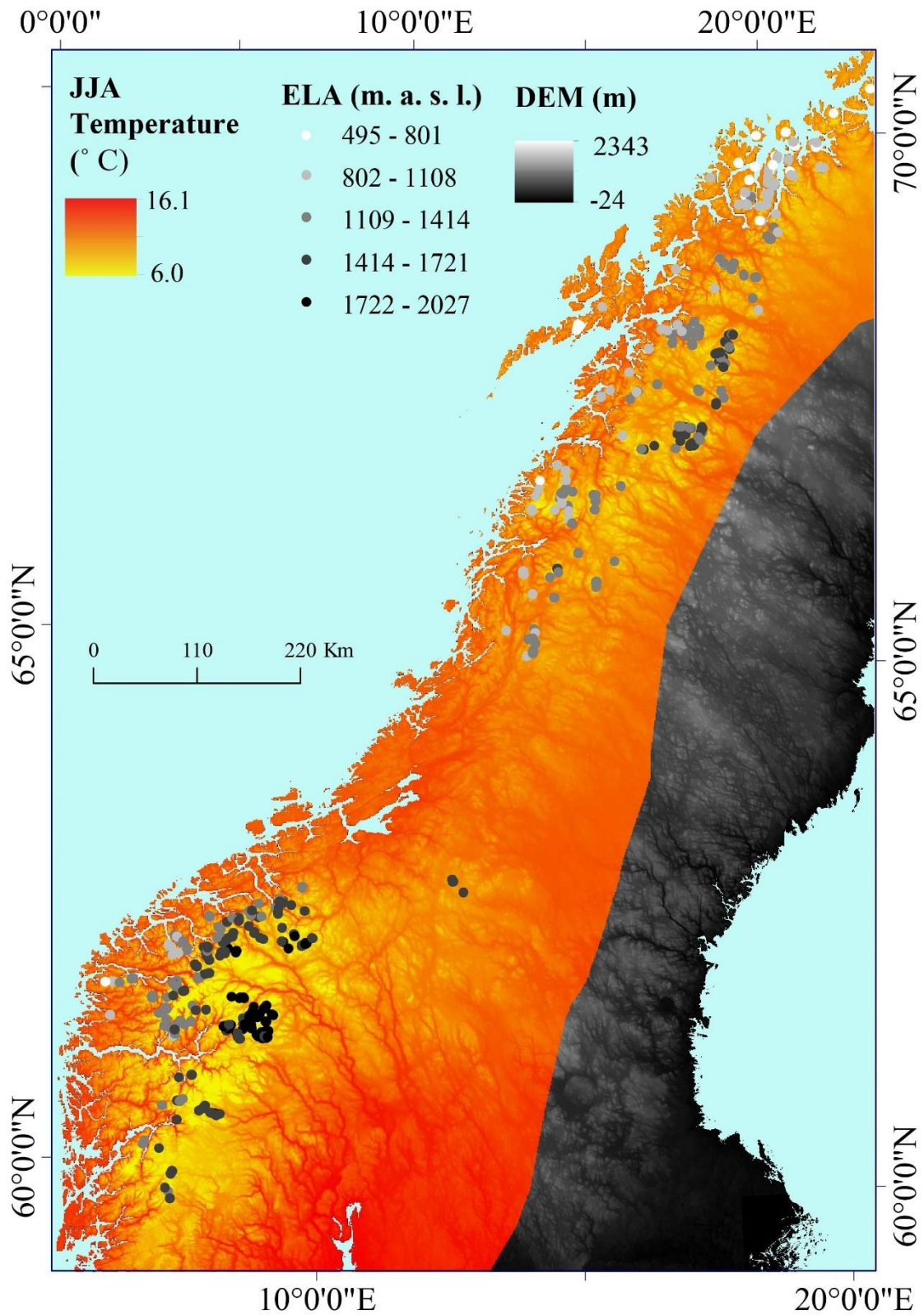
16

Figure 3: Present day (1976-2006) mean summer temperature (JJA) across the study area. Modern

cirque glacier ELAs are also shown. Climate data and DEM were obtained from the NVE.
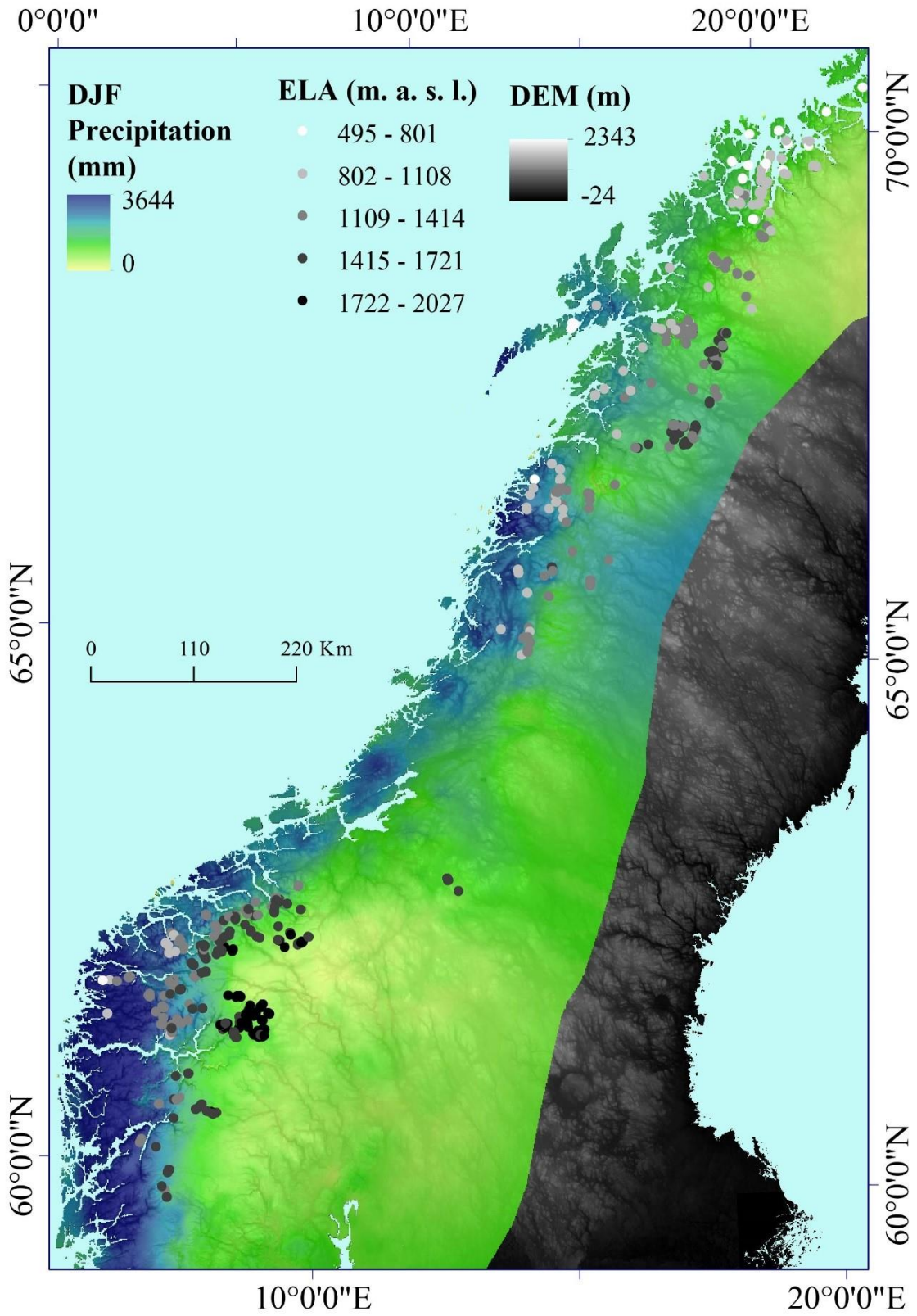
17

Figure 4:

Present day (1976-2006) winter precipitation across the study area. Modern cirque glacier ELAs are also shown. Climate data and DEM were obtained from the NVE.

	Solar Radiation	Latitude	Annual Precipitation	Winter Precipitation	Mean Annual Temperature	Distance to Coast	Mean Summer Temperature	Longitude
ELA (total)	0.347	-0.684	-0.187	-0.249	-0.667	0.817	-0.828	-0.585
North	0.159	-0.505	0.118	0.105	-0.853	0.788	-0.650	-0.224
South	0.277	-0.165	-0.783	-0.790	-0.878	0.741	-0.806	0.545

Table 1: Pearson correlations between ELA and topographic and climatic variables (at the ELA). All variables are statistically significant to 0.05. Dark grey shading represents 'very strong correlations, ± 0.75 - 1.0; medium grey 'strong' correlations, ± 0.5 - 0.749; light grey 'weak' correlations ± 0.25 - 0.499; and white 'very weak' correlations, ± 0.0 - 0.249.

	Latitude	Annual Precipitation	Winter Precipitation	Mean Annual Temperature	Distance to Coast	Mean Summer Temperature	Longitude
Distance to Coast (total)	-0.568	-0.266	-0.311	-0.668	-	-0.697	-0.414
North	-0.337	-0.142	-0.107	-0.843	-	-0.431	0.052
South	-0.514	-0.558	-0.582	-0.763	-	-0.643	0.445

Table 2: Pearson correlations between distance from the coast and other topographic and climatic variables at the cirque glacier ELA. All variables are statistically significant to 0.05. Shading to highlight correlation strength as for Table 1.
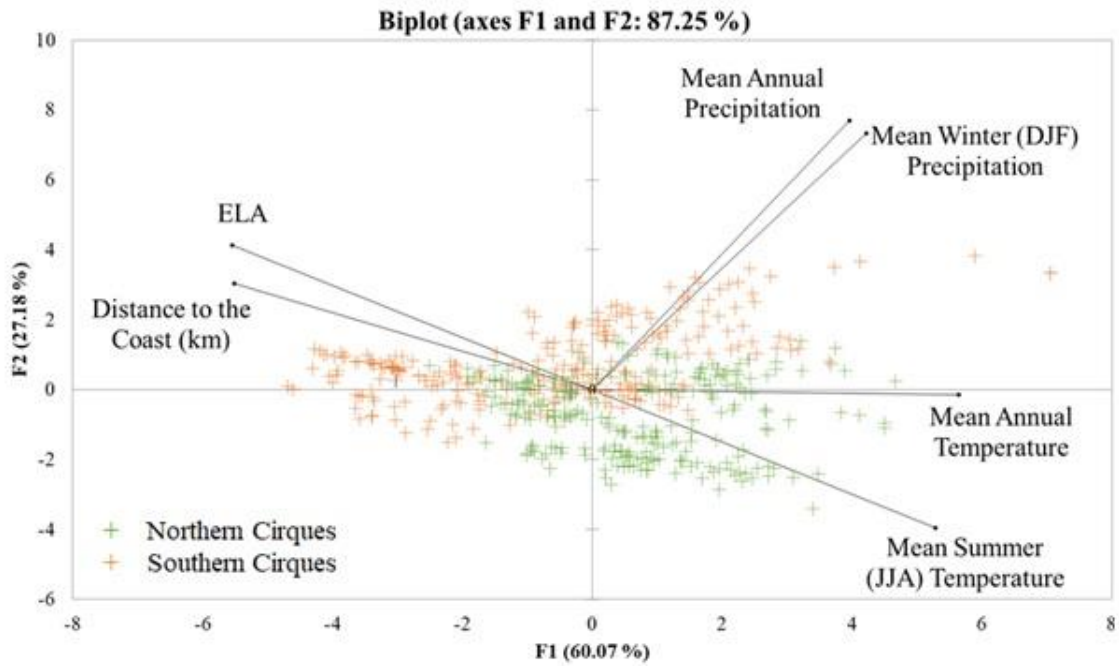
Figure 5: PCA of potential controls on Scandinavian cirque glacier ELAs. The orange crosses are the southern cirque glaciers and the green are the northern cirque glaciers. Northern cirque glaciers are distributed along the temperature component. Southern cirque glaciers are distributed along two components, precipitation and distance to coast, both reflecting the effect of continentality on southern cirque glacier distributions.
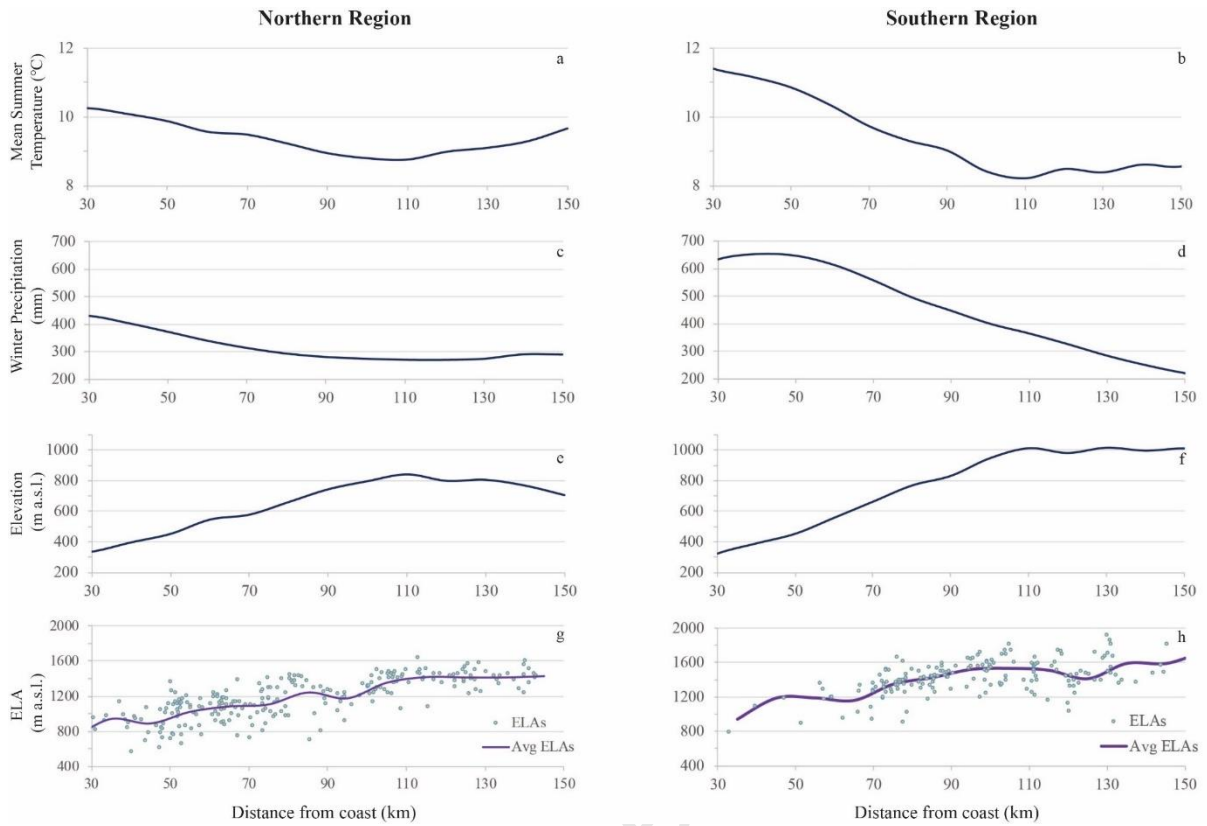
Figure 6: The plots show various trends with distance from the coast extracted within 10-km wide swaths that were generated parallel to the coast in both the south and north Scandinavia macro-regions: (a) mean summer air temperature in the northern region; (b) mean summer air temperature in the southern region; (c) winter precipitation in the northern region; (d) winter precipitation in the southern region; (e) mean topography in the northern region; (f) mean topography in the southern region; (g) average ELA in the northern region overlain with individual cirque glacier ELAs (blue dots); and (h) mean ELA in the southern region with individual cirque glacier ELAs.
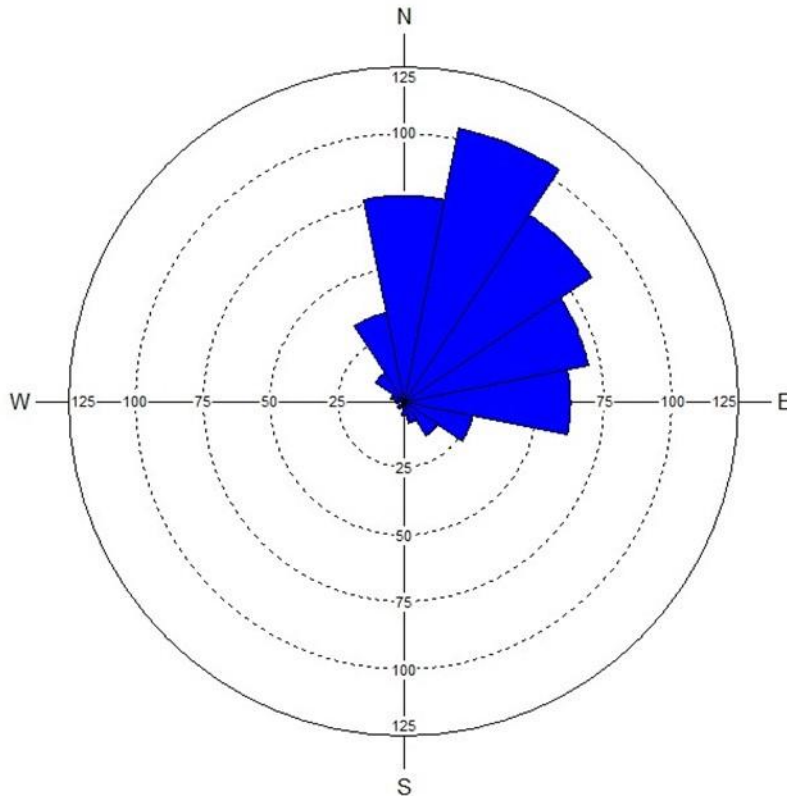
Figure 7: Rose diagram of cirque glacier mean aspect (n = 513). Each bin is 22.5°, (i.e. North spans 348.75 – 11.25) and the radius is the quantity of cirque glaciers that fall within that aspect bin. The mean direction of all cirque glacier aspects is 41°.

8.0 References

Anders, A. M., Mitchell, S. G. & Tomkin, J. H. Cirques, peaks, and precipitation patterns in the Swiss Alps: Connections among climate, glacial erosion, and topography. *Geology* **38**, 239–242 (2010).

Andreassen, L. M., Winsvold, S. H., Paul, F. & Hausberg, J. E. *Inventory of Norwegian glaciers. NVE Rapport* **38**, (2012).

Baker, P. A. Paleo-Precipitation Indicators. in *Encyclopedian of Earth Science Series: Encyclopedia of paleoclimatology and ancient environments* (ed. Gornitz, V.) **47**, 746–748 (2009).

Bakke, J., Trachsel, M., Kvisvik, B. C., Nesje, A., & Lyså, A. (2013). Numerical analyses of a multi-proxy data set from a distal glacier-fed lake, Sørsendalsvatn, western Norway. *Quaternary Science Reviews*. https://doi.org/10.1016/j.quascirev.2013.05.003

Barr, I. D. *et al.* Climate patterns during former periods of mountain glaciation in Britain and Ireland: Inferences from the cirque record. *Palaeogeogr. Palaeoclimatol. Palaeoecol.* **485**, 466–475 (2017).

Barr, I. D. & Spagnolo, M. Understanding controls on cirque floor altitudes: Insights from Kamchatka. *Geomorphology* **248**, 1–13 (2015a).

Barr, I. D. & Spagnolo, M. Glacial cirques as palaeoenvironmental indicators: Their potential and limitations. *Earth-Science Rev.* **151**, 48–78 (2015b).

Benn, Douglas I.; Lehmkuhl, F. Mass balance and equilibrium-line altitudes of glaciers in high-mountain environments. *Quat. Int.* **65/66**, 15–29 (2000).

Braithwaite, R. J. Can the mass balance of a glacier be estimated from its equilibrium-line altitude? *J. Glaciol.* **30**, 364–368 (1984).

Braithwaite, R. J. & Raper, S. C. B. Estimating equilibrium-line altitude (ELA) from glacier inventory data. *Ann. Glaciol.* **50**, 127–132 (2009).

Carrivick, J. L. & Brewer, T. R. Improving Local Estimations and Regional Trends of Glacier Equilibrium Line Altitudes. *Geogr. Ann. Ser. A Phys. Geogr.* **86**, 67–79 (2004).

Chueca, J. & Julián, A. Relationship between solar radiation and the development and morphology of small cirque glaciers (Maladeta Mountain massif, Central Pyrenees, Spain). *Geogr. Ann. Ser. A Phys. Geogr.* **86**, 81–89 (2004).

Engelhardt, M., Schuler, T. V. & Andreassen, L. M. Evaluation of gridded precipitation for Norway using glacier mass-balance measurements. *Geogr. Ann. Ser. A Phys. Geogr.* **94**, 501–509 (2012).

Evans, I. S. Glacier distribution and direction in Svalbard, Axel Heiberg Island and throughout the Arctic: General northward tendencies. *Polish Polar Res.* **32**, 199–238 (2011).

Evans, I. S. Local aspect asymmetry of mountain glaciation: A global survey of consistency of favoured directions for glacier numbers and altitudes. *Geomorphology* **73**, 166–184 (2006a).

Evans, I. S. Glacier Distribution in the Alps : Statistical Modelling of Altitude and Aspect. *Geogr. Ann. Ser. A Phys. Geogr.* **88 A**, 115–133 (2006b).

Evans, I. S. & Cox, N. Geomorphometry and the Operational Definition of Cirques. *R. Geogr. Soc. (with Inst. Br. Geogr.* **6**, 150–153 (1974).

Fujita, K. Effect of precipitation seasonality on climatic sensitivity of glacier mass balance. *Earth Planet. Sci. Lett.* **276**, 14–19 (2008).

GLIMS and NSIDC. Global Land Ice Measurements from Space glacier database. Compiled and made available by the international GLIMS community and the National Snow and Ice Data Center, Boulder CO, U.S.A. (2005, updated 2018).

Grudd, H. Small glaciers as sensitive indicators of climatic fluctuations. *Geogr. Ann. Ser. A* **72 A**, 119–123 (1990).

Hanssen-Bauer, I. Regional temperature and precipitation series for Norway: Analyses of time-series updated to 2004. *Report* (2005).

Hertzberg, J. E., Schmidt, M. W. & Sciences, A. Encyclopedia of Geochemistry. *Elements* **15**, 137–138 (2019).

Ipsen, H. A., Principato, S. M., Grube, R. E. & Lee, J. F. Spatial analysis of cirques from three regions of Iceland: implications for cirque formation and palaeoclimate. *Boreas* **47**, 565–576 (2018).

Jansen, H. L., Simonsen, J. R., Dahl, S. O., Bakke, J., & Nielsen, P. R. (2016). Holocene glacier and climate fluctuations of the maritime ice cap Høgtuvbreen, northern Norway. *The Holocene*, *26(5)*(736*755). https://doi.org/10.1177/0959683615618265

Kellogg, T. B. (1977). Paleoclimatology and paleo-oceanography of the Norwegian and Greenland Seas: The last 450,000 years. *Marine Micropaleontology*, *2*(C), 235–249. https://doi.org/10.1016/0377-8398(77)90013-5

Kjøllmoen, Bjarne (Ed.); Andreassen, Liss M.; Elvehoy, Hallgeir; Jackson, Miriam; Kjøllmoen, Bjarne; Melvold, K. *Glaciological investigations in Norway 2016*. *Norwegian Water Resources and Energy Directorate* (Norwegian Water Resources and Energy Directorate, 2017).

Křížek, M. & Mida, P. The influence of aspect and altitude on the size, shape and spatial distribution of glacial cirques in the High Tatras (Slovakia, Poland). *Geomorphology* **198**, 57–68 (2013).

Lauritzen, S.-E. (1995). High-Resolution Paleotemperature Proxy Record for the Last Interglaciation Based on Norwegian Speleothems. *Quaternary Research*, *43*, 133–146.

Lussana, C., Tveito, O. E., Uboldi, F. & Cristian, L. *seNorge v2.0, Temperature An observational gridded dataset of temperature for Norway METreport Title Date seNorge v2.0: an observational gridded dataset of temper-ature for Norway*. *Norwegian Meterological Institute* (2016).

Mangerud, J., Nstegaard, S. ", Sejrup, H.-P., & Haldorsen, S. (1981). A continuous Eemian-Early Weichselian sequence containing pollen and marine fossils at Fjpsanger, western Norwav. *Boreas*, *10*, 137–208.

Nesje, A. (2009). Latest Pleistocene and Holocene alpine glacier fluctuations in Scandinavia. *Quaternary Science Reviews*, *28*(21–22), 2119–2136. https://doi.org/10.1016/j.quascirev.2008.12.016

Nesje, A. Topographical Effects on the Equilibrium Line Altitude on Glaciers. *GeoJournal* **27**, 383–391 (1992).

Nesje, A., Bakke, J., Dahl, S. O., Lie, Ø., & Matthews, J. A. (2008). Norwegian mountain glaciers in the past, present and future. *Global and Planetary Change*, *60*(1–2), 10–27. https://doi.org/10.1016/j.gloplacha.2006.08.004

Norwegian Mapping Authority. The Terrain Model WMS Service Provides Information on the Terrestrial Terrain Model (DTM 10). https://www.kartverket.no/data/Laserskanning/(2016).

NVE. Norwegian Water Resources and Energy Directorate (NVE). Climate indicator products, http://glacier.nve.no/viewer/CI/, downloaded <2017.12.01>. (2017).

Oerlemans, J. & Hoogendoorn, N. C. Mass-balance gradients and climatic change. *J. Glaciol.* **35**, 399–405 (1989).

Ohmura, A. & Boettcher, M. Climate on the equilibrium line altitudes of glaciers: Theoretical background behind Ahlmann's P/T diagram. *J. Glaciol.* **64**, 489–505 (2018).

Ohmura, A. ; Kasser, P. ; Funk, M. Climate at the equilibrium line of glaciers. *J. Glaciol.* **38**, 397–411 (1992).

Olsen, L., Sveian, H., Ottesen, D. and Rise, L. (2013) Quaternary glacial, interglacial and interstadial deposits of Norway and adjacent onshore and offshore areas. In Olsen, L., Fredin, O. and Olesen, O. (eds.) *Quaternary Geology of Norway*, Geological Survey of Norway Special Publication, 13, pp. 79–144

Osmaston, H. (2005). Estimates of glacier equilibrium line altitudes by the Area × Altitude, the Area × Altitude Balance Ratio and the Area × Altitude Balance Index methods and their validation. *Quaternary International*, *138–139*, 22–31. https://doi.org/10.1016/j.quaint.2005.02.004

Pearce, D. M., Ely, J. C., Barr, I. D. & Boston, C. M. Section 3.4.9: Glacier Reconstruction. in *Geomorphological Techniques (Online Edition)* **9**, (British Society for Geomorphology, 2017).

Pellitero, R. *et al.* A GIS tool for automatic calculation of glacier equilibrium-line altitudes. *Comput. Geosci.* **82**, 55–62 (2015).

Raper, S. C. B. & Braithwaite, R. J. Glacier volume response time and its links to climate and topography based on a conceptual model of glacier hypsometry. *Cryosphere* **3**, 183–194 (2009).

Raup, B. *et al.* The GLIMS geospatial glacier database: A new tool for studying glacier change. *Glob. Planet. Change* **56**, 101–110 (2007).

Rea, B. R. Defining modern day Area-Altitude Balance Ratios (AABRs) and their use in glacier-climate reconstructions. *Quat. Sci. Rev.* **28**, 237–248 (2009).

Rosqvist, G. & Østrem, G. The Sensitivity of a Small Icecap to Climatic Fluctuations. *Geogr. Ann. Ser. A Phys. Geogr.* **71**, 99–103 (1989).

Rudberg, S. Glacial cirques in Scandinavia. *Nor. Geogr. Tidsskr. - Nor. J. Geogr.* **48**, 179–197 (1994).

Rupper, S. & Roe, G. Glacier changes and regional climate: A mass and energy balance approach. *J. Clim.* **21**, 5384–5401 (2008).

Sagredo, E. A., Rupper, S. & Lowell, T. V. Sensitivities of the equilibrium line altitude to temperature and precipitation changes along the Andes. *Quat. Res. (United States)* **81**, 355–366 (2014).

Skoglund, R. Ø., & Lauritzen, S.-E. (2010). Morphology and speleogenesis of Okshola, Fauske, northern Norway: example of a multi-stage network cave in a glacial landscape. In *Norwegian Journal of Geology* (Vol. 90).Spagnolo, M. *et al.* ACME, a GIS tool for Automated Cirque Metric Extraction. *Geomorphology* **278**, 280–286 (2017).

Sutherland, D. G. Modern glacier characteristics as a basis for inferring former climates with particular reference to the Loch Lomond Stadial. *Quat. Sci. Rev.* **3**, 291–309 (1984).

Torsnes, I., Rye, N., & Nesje, A. (1993). Arctic and Alpine Research Modern and Little Ice Age Equilibrium-line Altitudes on Outlet Valley Glaciers from Jostedalsbreen, Western Norway: An Evaluation of Different Approaches to their Calculation. *Arctic and Alpine Research*, *25*(2), 106–116. https://doi.org/10.1080/00040851.1993.12002990

Trachsel, M. & Nesje, A. Modelling annual mass balances of eight Scandinavian glaciers using statistical models. *Cryosphere* **9**, 1401–1414 (2015).

Trenhaile, A. S. Cirque Morphometry in the Canadian Cordillera Author. *Ann. Assocation Am. Geogr.* **66**, 517–529 (1975).

Tveito, O. E. *et al. DNMI - Nordic temperature maps*. *DNMI - Report* **09/00 KLIM**, (Norwegian Meterological Institute, 2000).

WGMS. Fluctuations of Glaciers Database. World Glacier Monitoring Service, Zurich, Switzerland. DOI:10.5904/wgms-fog-2018-11. Online access: http://dx.doi.org/10.5904/wgms-fog-2018-11. (2018).

WGMS, and National Snow and Ice Data Center (comps.). World Glacier Inventory, Version 1. Boulder, Colorado USA. NSIDC: National Snow and Ice Data Center. DOI:

https://doi.org/10.7265/N5/NSIDC-WGI-2012-02. [24 October 2018. (1999). updated 2012.

Winkler, S., Elvehy, H. & Nesje, A. Glacier fluctuations of Jostedalsbreen, western Norway, during the past 20 years: The sensitive response of maritime mountain glaciers. *Holocene* **19**, 395–414 (2009).

Winkler, S. & Nesje, A. Perturbation of climatic response at maritime glaciers? *Erdkunde* **63**, 229–244 (2009).

Winsvold, S. H., Andreassen, L. M. & Kienholz, C. Glacier area and length changes in Norway from repeat inventories. *Cryosphere* **8**, 1885–1903 (2014).

Wong, W. K., Haddeland, I., Lawrence, D. & Beldring, S. Gridded 1 x 1 km climate and hydrological projections for Norway. 25 (2016).

Declaration of interests

28

☒ The authors declare that they have no known competing financial interests or personal relationships that could have appeared to influence the work reported in this paper.

☐The authors declare the following financial interests/personal relationships which may be considered as potential competing interests:

Declaration of interests

Highlights

- Distance from the coast affects ELA differently in the S and N Scandinavian regions. This reflects the competing effect of temperature and precipitation on glacier ELA.

- When assessing the relationship between climatic and ELA trends, the extent of the study area is of paramount importance.

- When un-occupied (ice-free) cirques are analysed for palaeoclimatological reconstruction, the time transgressive nature of cirque occupation must be considered.

- Topographic availability matters: if there is no topography at the theoretical ELA, glaciers cannot form, and this might affect apparent ELA-climatic gradients.